OPEN

NPG Asia Materials (2015) 7, e224; doi:10.1038/am.2015.120
www.nature.com/am

ORIGINAL ARTICLE

One-step, continuous synthesis of a spherical $Li_4Ti_5O_{12}$/graphene composite as an ultra-long cycle life lithium-ion battery anode

Shun Mao[1], Xingkang Huang[1], Jingbo Chang, Shumao Cui, Guihua Zhou and Junhong Chen

We report, for the first time, a one-step, continuous synthesis of spherical lithium titanate ($Li_4Ti_5O_{12}$, LTO)/graphene composites through direct aerosolization of a graphene oxide (GO) suspension mixed with Li and Ti precursors. The resulting crumpled graphene-sphere-supported LTO nanocrystals has a three-dimensional structure with a high electrical conductivity, a high surface area and good stability in electrolyte. The LTO/CG composite, as an anode in LIBs, exhibited excellent rate capability (for example, at a high current density of 5000 mA g^{-1} it delivered 60% of the capacity obtained at 12.5 mA g^{-1}) and an outstanding cycling performance (a capacity retention of 88% after 5000 cycles at 1,250 mA g^{-1}). The one-step, continuous synthesis of the LTO/graphene composite offers a high-producing efficiency compared with conventional multi-step preparations, and can be generally applied for synthesizing lithium metal oxides/graphene (cathode or anode) materials for lithium-ion batteries.

NPG Asia Materials (2015) **7**, e224; doi:10.1038/am.2015.120; published online 6 November 2015

INTRODUCTION

Lithium-ion batteries (LIBs) have a high-rate capacity and long cycle life, and thus are critical for many important applications, such as electric vehicles (EVs) and portable electronic devices.[1–3] The use of combustible graphite (especially in lithiated states) is highly risky in the application of EVs and hybrid EVs (HEVs); therefore, alternative anode materials with a higher power density, better stability, and higher safety performance are greatly needed and deserve greater scientific exploration.

Compared with graphitic carbon, spinel lithium titanate $Li_4Ti_5O_{12}$ (LTO) exhibits a relatively high lithium insertion/extraction voltage of ~1.55 V (vs Li^+/Li), which prevents the formation of the solid electrolyte interphase (SEI) and suppresses lithium dendrite deposition on the surface of the anode (most electrolyte materials or solvents are reduced below 1 V), thereby greatly decreasing the short-circuit risk of the battery.[4–8] In addition, LTO possesses excellent Li ion insertion and removal reversibility with almost zero volume change during the charge/discharge process.[9,10] However, as demonstrated in previous studies, it is still a challenge to achieve good battery performance at high charge/discharge rates using LTO as the anode material because of the low electrical conductivity ($<10^{-13}$ S cm^{-1}) of LTO,[11,12] and thus there have been many efforts to improve the rate capability and the cycling performance of LTO-based batteries. Commonly applied strategies include engineering the proper LTO structure to reduce the transport path length of Li ions and enhancing the electrical conductivity by surface coating or forming composites with carbon-based materials. Along these strategies, LTO has been fabricated into various nanostructures, for example, nanoparticles,[6,8,13] nanofibers/nanowires,[14,15] nanosheets[16,17] and porous networks,[7,10] or integrated with highly conductive carbons.[11,18–20]

Because graphene has excellent electrical conductivity, LTO/graphene composites have received significant attention lately. Xiang *et al.*[21] synthesized an LTO/graphene composite through a sol–gel method using lithium acetate, tetrabutyl titanate and graphene sheets; however, the capacity of as-obtained LTO/graphene decayed from 146 to 110 mAh g^{-1} within 100 cycles at a 10 C rate, which may be due to the difficulties with controlling the morphology of LTO/graphene from the sol–gel method. To better control the morphology of LTO/graphene, TiO_2/graphene oxide (GO) was synthesized as a precursor for LTO/GO. For example, Shen *et al.*[19] employed a three-step method with the hydrolysis of tetrabutyl titanate in the presence of GO to produce TiO_2/GO, which was then transformed into Li–Ti–O/reduced GO (RGO) by a hydrothermal process, and finally to LTO/RGO by a post-annealing process. Kim *et al.*[22] used a similar microwave assisted, two-step method with titanium ethoxide, LiOH and GO to obtain Li–Ti–O/RGO, which was then transformed to LTO/RGO by post annealing. Although these efforts have improved performance, it still remains a great challenge to fabricate LTO/graphene anodes with desirable architectures for achieving the high-rate capability and long cycle life of batteries. In addition, the multi-step synthesis increases the cost and limits the large-scale application

Department of Mechanical Engineering, University of Wisconsin-Milwaukee, Milwaukee, WI, USA
[1]These authors contributed equally to this work.
Correspondence: Professor J Chen, Department of Mechanical Engineering, University of Wisconsin-Milwaukee, 3200 North Cramer Street, Milwaukee, WI 53211, USA.
E-mail: jhchen@uwm.edu
Received 3 May 2015; revised 2 July 2015; accepted 20 September 2015

of LTO anodes, and a one-step, low-cost continuous preparation of LTO/graphene composite has not been reported.

Here we report on the one-step continuous preparation of spherical LTO/graphene composites through aerosolization of a GO suspension mixed with titanium(IV) bis(ammonium lactato) dihydroxide and LiOH precursors. The GO sheet was crumpled into a spherical shape when the GO-contained aerosol droplets flied through the high-temperature tube furnace; meanwhile, the Li and Ti precursor reacted, resulting in LTO nanocrystals distributed on the crumpled graphene (CG) sphere. The novelty in the present method is that LTO nanocrystals are locally crystallized and grown *in situ* on the surface of CG spheres during the solvent evaporation and GO crumpling process, leading to a highly stable hierarchical structure with LTO nanocrystals well distributed on the CG sphere. This type of architecture greatly improves the conductivity of the LTO and facilitates the electron/charge transfer between the anode materials and the current collector. This is the first report using an aerosolization method to produce LTO/graphene composites as an LIB anode.[23,24] More importantly, this method is a facile one-step process with no need for subsequent treatment of the product LTO/CG; therefore, the method is suitable for continuous production and thus promising for large-scale manufacturing. In addition, the spherical morphology of the LTO/CG favors a higher tap density for practical LIB applications. As demonstrated in the battery test, LIBs with LTO/CG composites as the anode exhibited an excellent rate capability and an ultra-long cycle life.

EXPERIMENTAL PROCEDURES

Synthesis of LTO/CG hybrids

The LTO/CG hybrid was produced by a previously reported aerosolization/high-temperature-induced GO crumpling and nanocrystal growth method (Supplementary Information, Supplementary Figure S1). In a typical procedure, 50-ml GO suspension (0.3 mg ml^{-1} in deionized water) was mixed with titanium(IV) bis(ammonium lactato) dihydroxide (0.25 ml, 50 wt.% solution in water, Sigma-Aldrich, St Louis, MO, USA) and LiOH (9.1 mg, Sigma-Aldrich). The amount of Ti and Li precursors were determined according to the stoichiometry of Ti and Li in LTO. However, based on our experiments, 100% LiOH will lead to TiO_2 in the final product due to the different adsorption and evaporation properties of the Ti and Li precursors in the aerosolization process. To eliminate the TiO_2, excessive LiOH (110 and 130%) was used and it was found that, with 130% LiOH, pure LTO/CG could be produced without any TiO_2. The mixed solution was nebulized by an ultrasonic nebulizer (2.4 MHz, 241T, Sonaer) to form aerosol particles, which were carried by argon gas through a horizontal tube furnace preheated at a desired temperature (750 °C). The GO sheets were quickly dried and crumpled while traveling in the tube furnace, and the precursors adsorbed on the GO surface reacted to the form LTO nanocrystals. The produced LTO/CG (black powders) were collected with a filter paper at the outlet and used without any further treatment.

LTO/CG characterization

The morphology/structure of the LTO/CG hybrids were studied using a Hitachi (Tokyo, Japan; H 9000 NAR) transmission electron microscope (TEM) and a Hitachi (S-4800) scanning electron microscope (SEM) equipped with an energy-dispersive spectroscopy analyzer. Powder X-ray diffraction was performed on a Scintag XDS 2000 diffractometer (Scintag, Inc., Sunnyvale, CA, USA) with Cu Kα radiation; the data were collected between scattering angles (2θ) of 10 and 70°. Raman spectroscopy was conducted with a Renishaw Raman spectrometer (Renishaw Inc., Wotton-under-Edge, UK; Inc 1000B) with an HeNe laser. Thermogravimetric/differential thermal analysis was carried out under air flow (100 ml min^{-1}) at a heating rate of 5 °C min^{-1} on a SDT 2660 Simultaneous DSC-TGA instrument (TA Instruments, New Castle, DE, USA). The tap density of the LTO/CG was measured according to the standard test method for determination of tap density of metallic powders and compounds (ASTM B527–06), where we used a 1-mL measuring pipette instead of a 25-mL graduated glass cylinder because of the limited sample amount.

Battery measurements

The charge/discharge performance was characterized by using 2032-type coin cells that were assembled in an argon-filled glove box with contents of oxygen and moisture below 1 p.p.m. Electrodes were prepared by mixing the as-prepared LTO/CG as the active material, and poly(acrylic acid) as a binder, and carbon black as a conductor with a weight ratio of 70:15:15 to form a slurry. The resulting slurries were coated onto a Cu foil (12 μm in thickness) current collector by using the doctor-blade method. After drying and pressing, the Cu foil was cut into disks (1.11 cm in diameter) with typical electrode material loadings of ca. 1 mg cm^{-2}. Then, 1M $LiPF_6$ dissolved in ethylene carbonate/ethyl methyl carbonate (40:60, v/v) was employed as an electrolyte.

Electrochemical test

Cyclic voltammetry (CV) and electrochemical impedance spectroscopy of the as-prepared anodes were measured on a PARSTAT 4000 electrochemical station (Princeton Applied Research, Oak Ridge, TN, USA) using a three-electrode cell, with the LTO/CG electrode as a working electrode, a lithium disk as a counter electrode, and a lithium ring as a reference electrode. CV was carried out at a scanning rate of 0.05 mV s^{-1}, whereas electrochemical impedance spectroscopy was tested between 10,000–0.1 Hz with an amplitude of 10 mV.

RESULTS AND DISCUSSION

LTO/CG composite synthesis through aerosolization method

The LTO/CG hybrid was produced by an aerosolization/high-temperature-induced GO crumpling and nanocrystal growth method. Recently, CG has drawn increasing attention due to its three-dimensional (3D) hollow structure and excellent stability in aqueous solutions.[25–27] Furthermore, due to its highly conductive nature and large specific surface area, the CG is a promising substrate for loading active materials into energy devices, that is, supercapacitors[24,28,29] and batteries,[30–34] and as a catalyst support in fuel cells.[23] As shown in Figure 1, the GO suspension was first mixed with precursors (titanium (IV) bis(ammonium lactato) dihydroxide and LiOH) and then nebulized to generate aerosol droplets, which flowed through a tube

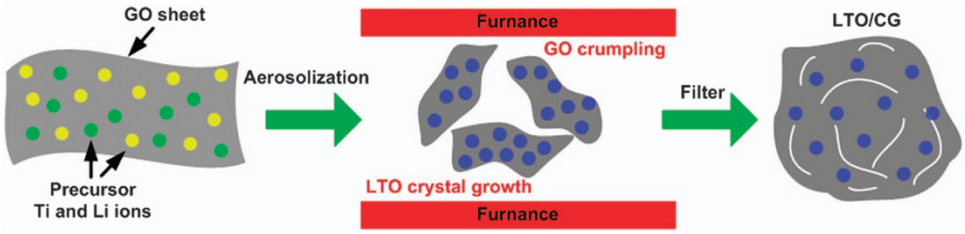

Figure 1 Preparation of LTO/CG hybrids by rapid compression of GO sheets in evaporating aerosol droplets and simultaneous chemical reaction to grow LTO nanocrystals on the CG surface. GO, graphene oxide; LTO/CG, $Li_4Ti_5O_{12}$/crumpled graphene.

furnace. Because of the rapid evaporation of the solvents, the GO sheets were compressed into a crumpled sphere shape while LTO nanocrystals were simultaneously grown from precursors and assembled on the surface of graphene spheres. Notably, this is the first study using two precursor ions mixed with GO to produce CG/nanocrystal composites through the aerosolization method, thereby expanding its capability to synthesize CG-based composites. The product graphene spheres have a rigid structure and high resistivity under compression and is stable in aqueous solutions. This type of CG sphere also has a large specific surface area (up to 587 $m^2 g^{-1}$)[25] and is highly conductive due to the efficient reduction of GO from heating in the furnace.[35]

The LTO/CG hybrid was first characterized by SEM and TEM images (Figure 2). The SEM images show that the LTO/CG hybrid has a spherical shape and small LTO nanocrystals are uniformly deposited on the surface of CG spheres. This structure is very similar to our previously reported nanocrystal/CG hybrids (Mn_3O_4/CG and SnO_2/CG).[24] The hybrid spheres have a relatively wide size distribution, ranging from dozens to a few hundred nanometers, which is mainly dependent on the original size of the GO sheets. The spherical morphology is favored for industry because it benefits a high tap density. The tap density of the LTO/CG composite was measured to be 1.5 g cm^{-3}, meeting the requirement for the practical application. As expected, the graphene sphere has a 3D hollow structure and nanocrystals are deposited on both sides of the graphene, which is clearly evidenced in the TEM image shown in Figure 2d. The TEM image also reveals the LTO nanocrystals are closely packed on the graphene surface, with a diameter of a few nanometers (5–10 nm). The high-resolution TEM image and selected area electron diffraction patterns (Figures 2e and c, respectively) confirm that the LTO nanocrystals have a well-defined crystalline structure. The major lattice spacing of LTO nanocrystals is measured at 0.484 nm, which matches well with the *d*-spacing of LTO (111).

To further investigate the composition of the hybrids, energy-dispersive X-ray spectroscopy elemental mapping of the LTO/CG hybrid was performed (Supplementary Information,Supplementary Figure S2). The titanium, carbon, and oxygen elements are clearly seen in the mapping data of the LTO/CG and the signals match well with the composite spheres shown in the corresponding SEM image, further suggesting the hybrid is constructed by LTO nanocrystals and graphene. X-ray diffraction spectroscopy presents additional information on the crystallographic structure of the LTO/CG hybrid. Initially, to prepare the LTO/CG composite, the amount of Ti and Li precursors were determined according to the stoichiometry of Ti and Li in LTO. However, based on our experiments, 100% LiOH led to TiO_2 in the final product due to the different adsorption and evaporation properties of Ti and Li precursors in the GO aerosolization process. To eliminate the TiO_2, excess LiOH (by 10 and 30%)

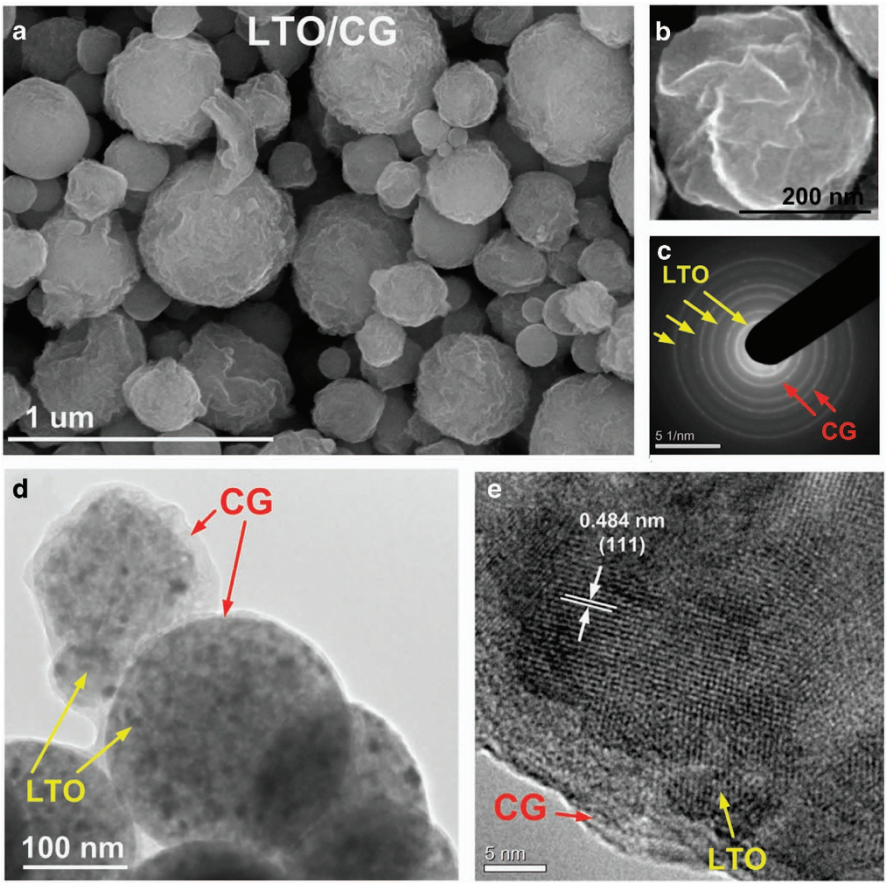

Figure 2 (**a**) and (**b**) SEM images of the LTO/CG hybrids. Graphene nanosheets were crumpled into a spherical shape with LTO nanocrystals decorated on the surface. (**d**) TEM image of the LTO/CG hybrids. LTO nanocrystals were found to be a few nanometers in size. (**e**) and (**c**) HRTEM image and SAED patterns of the LTO/CG hybrids. HRTEM, high-resolution TEM; LTO/CG, $Li_4Ti_5O_{12}$/crumpled graphene; SAED, selected area electron diffraction; SEM, scanning electron microscope.

was used and it was found that, with 130% LiOH, pure LTO/CG could be produced without any TiO_2. The X-ray diffraction pattern of the LTO/CG produced with 130% LiOH (Supplementary Information, Supplementary Figure S3a) shows sharp diffraction peaks corresponding with (111), (311), (400), (331), (333), (440) and (531) crystal facets from cubic LTO without any detectable impurity phases. In comparison, the X-ray diffraction pattern of LTO/CG produced with 110% LiOH (Supplementary Information, Supplementary Figure S3b) has small diffraction peaks from anatase TiO_2, indicating the excess amount of the LiOH is critical for preparing pure LTO/CG composite using the aerosolization method.

The structure configurations of GO and LTO/CG samples were further investigated with Raman spectroscopy, as shown in the Supplementary Information, Supplementary Figure S4a. Typical bands from graphene-related materials are found in both spectra, that is, the G band (~1595 cm^{-1}) from the sp^2 carbon, the D band (~1332 cm^{-1}) from structural imperfections in the graphene sheet, and two-dimensional band (~2665 cm^{-1}) from graphitic carbon in the graphene-like materials.[36] The Raman spectra show that the ratio of I_D/I_G increased after the GO transformed to CG due to the increased fraction of crumples in CG. The increased I_D/I_G ratio is also attributed to the increased number of defect-free sp^2 carbons, which formed smaller domains than those in GO (large quantities of structural defects) after reduction.[37,38] The Raman results indicate the CG in LTO/CG is actually RGO, which is consistent with previous results of CG under various crumpling temperatures.[35] To study the graphene content in the hybrids, thermogravimetric analysis was performed (Supplementary Information, Supplementary Figure S4b) and the results show that about 6.5% of the sample weight was lost when the sample was heated to 750 °C, indicating the graphene content in the hybrid is around 6.5 wt.%.

Battery performance of the LTO/CG anode

The batteries were fabricated by using the LTO/CG composites (pure LTO/CG from 130% LiOH) as the anode and then assembled and tested in a coin cell device with a metallic lithium counter electrode. Figure 3 exhibits the charge/discharge performance of the LTO/CG composite. The voltage range was limited between 1.0 and 2.0 V, so that graphene was inactive and served only as a conducting component. The specific capacity values reported in Figure 3 were calculated on the basis of the total weight of LTO and CG in the LTO/CG composites, in which LTO comprises 93.5 wt.% of the total mass. The

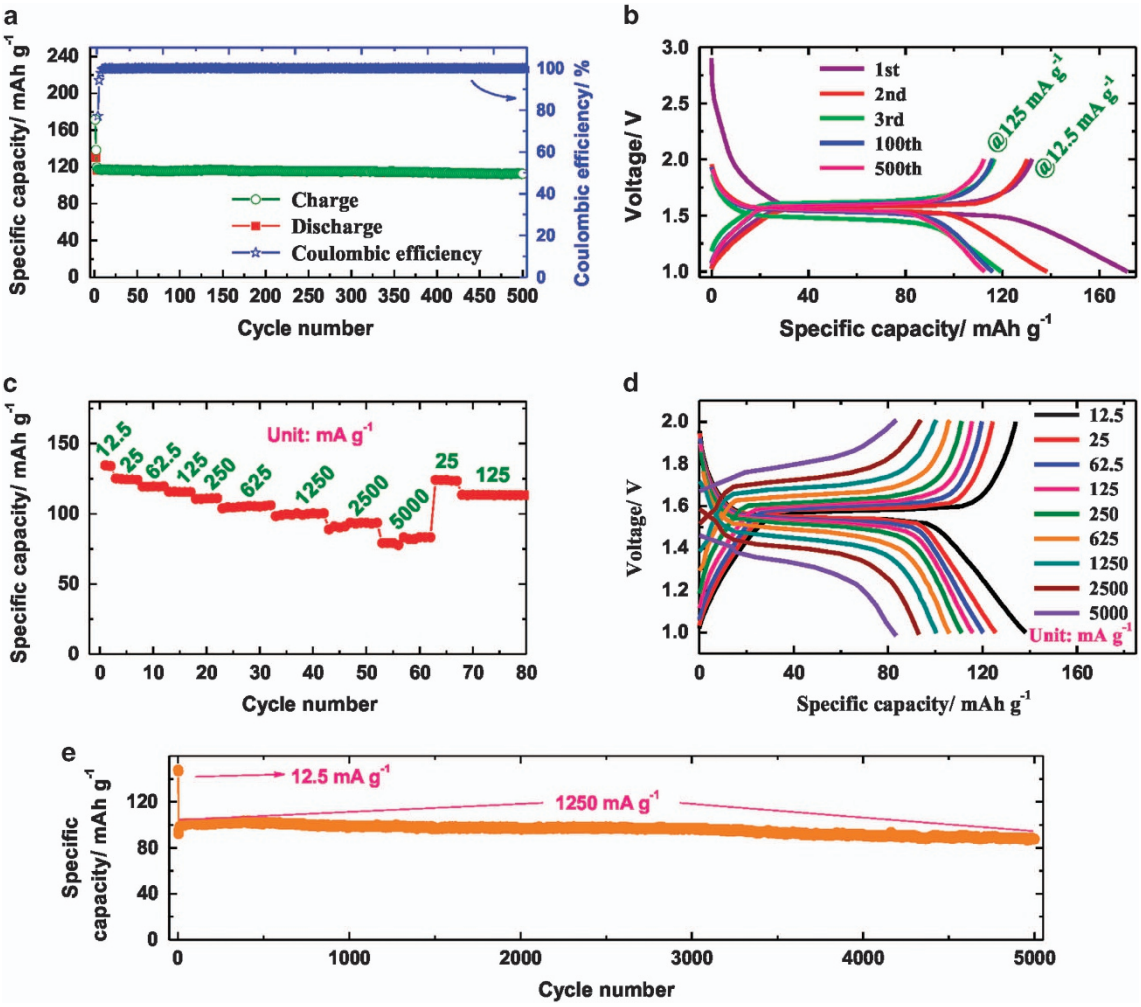

Figure 3 Battery performance of the LTO/CG anode. Electrochemical performance of the LTO/CG composite within the voltage range of 1–2 V: (**a**) cyclic performance at a current density of 125 mA g^{-1} after activation during the initial two cycles at 12.5 mA g^{-1}, (**b**) charge/discharge curves, (**c**, **d**) rate capability, and (**e**) long-life cycling at 1250 mA g^{-1}. LTO/CG, $Li_4Ti_5O_{12}$/crumpled graphene.

LTO/CG was activated for two cycles at a current density of 12.5 mA g^{-1}, showing a capacity of ca. 140 mAh g^{-1} and then cycled at 125 mA g^{-1}, delivering a capacity of ca. 120 mAh g^{-1} over 500 cycles (Figures 3a and b). The LTO/CG exhibited excellent rate capability, as shown in Figures 3c and d, at a very high current density of 5000 mA g^{-1}; the LTO/CG composite delivered a capacity of ca. 83 mAh g^{-1}, corresponding with 60% of the capacity obtained at 12.5 mA g^{-1}. The LTO/CG was cycled at 1,250 mA g^{-1} to evaluate its cycle performance, showing a capacity of ca. 100 mAh g^{-1} and retaining 88 mAh g^{-1} after 5000 cycles. Note that the initial Coulombic efficiency is 77 % (Figure 3a), which is believed to be related to the irreversible capture of lithium ions by oxygen groups on the graphene surfaces. Shi *et al.*[39]reported that the increased graphene content in LTO/graphene composite could lead to a decreased initial Coulombic efficiency. In their study, compared with the initial Coulombic efficiency of 94.5% for the pristine LTO, the value decreased to 90.0 and 85.7% for the 5 and 10 wt.% graphene in the LTO/graphene composites, respectively.

As we discussed, many different methods have been applied to synthesize LTO/graphene composites for LIB anode. For example, Shen *et al.*[19] prepared an LTO/RGO composite through the hydrolysis of tetrabutyl titanate and GO to form TiO_2/GO, followed by a hydrothermal treatment in the presence of LiOH and hydrazine hydrate and post annealing. The as-obtained LTO/RGO delivered a capacity of 171.4 and 82.7 mAh g^{-1} (based on the LTO mass) at 0.1 and 60 C rates (in this case, 1 C was defined as 170 mAh g^{-1}), respectively, showing good rate capability. LTO/RGO composites have been synthesized and widely investigated using a similar approach.[22,40–43] The typical performance of LTO/RGO anodes from this method includes 144 mAh g^{-1} at 10C (retained 85% after 2000 cycles)[40] and 162 mAh g^{-1} at 10C (retained 90.7% after 500 cycles).[43] Another method for preparing LTO/RGO composite, as reported by Oh *et al.*[44] is wrapping GO sheets onto a TiO_2 (P25) particle, followed by annealing in the presence of Li_2CO_3. LTO/RGO composites prepared with this method also exhibited good rate capability, for example, delivering ~105 mAh g^{-1} at 100C. Compared with these LTO/RGO composites, our LTO/CG composite exhibited superior performance in both rate capability and cyclability. Specifically, at a high current density of 5000 mA g^{-1} (28.6 C if 1 C is defined as 175 mAh g^{-1}), the LTO/CG composite delivered a capacity of ca. 83 mAh g^{-1}, which is 60% of the capacity obtained at 12.5 mA g^{-1}, and retaining 88% of the reversible capacity after 5000 cycles. More importantly, compared with these LTO/RGO composites synthesized through multiple steps (at least four steps if including washing and drying), our LTO/CG was continuously fabricated in one-step with no need for post-treatment.

Note that 1 C was typically defined as 175 mAh g^{-1}, which is the theoretical capacity of LTO when lithiating to $Li_7Ti_5O_{12}$ (above 1.0 V); however, 1 C-rate, according to industry standards, is the current to discharge an entire battery in 1 h; and the resulting capacity is 1 C capacity. For example, our LTO/CG composite delivered ca. 120 mAh g^{-1} at 125 mA g^{-1} (1.0–2.0 V), suggesting the 1 C capacity as 120 mAh g^{-1} that can be used on designing a full cell. Thus, the 1 C-rate can be defined as 120 mA g^{-1} for our LTO/CG composite and the highest current density of 5000 mA g^{-1} corresponds with 41.7 C, indicating that our LTO/CG composite meets the requirement for the LIB applications for EV and HEV (typically 2–20 C).

The excellent rate capability and outstanding cycling performance of the LTO/CG anode are due to the unique structure of the LTO/CG composite. First, LTO nanocrystals with a small size and a high specific surface area can offer a short pathway for lithium transport and resections, which leads to better rate (power) performance. Second, the composite structure of LTO nanocrystals decorated on the surface of CG can effectively prevent aggregation of the nanocrystals. The 3D hollow graphene structure offers ample space for the possible structure change of LTO upon lithiation, which is beneficial for maintaining the stability of the LTO anode and improving its cyclability. Third, the CG support provides a conductive network for electronic transport, which improves the electrical conductivity, rate capability, and usage of LTO nanocrystals. Finally, since the LTO nanocrystals were grown *in situ* on the graphene surface, the strong binding between the two materials prevents the detachment of the LTO nanocrystals from the current collector, which improves the stability of the anode. To confirm the stability of the LTO/CG anode during the lithiation/delithiation processes, SEM images were used to study the structure of the composite anode before and after cycling tests. As shown in Supplementary Figure S5, there is no obvious change in the LTO/CG structure and no LTO nanocrystal loss is found after 500 cycles between 1 and 2 V at 125 mA g^{-1}. This further confirms that the outstanding cycling performance of the LTO/CG anode is due to the highly stable LTO/CG structure.

Considering graphene as an active anode material, the batteries were also tested with an extended lower voltage cutoff at 0.01 V, and the electrochemical performance of the LTO/CG composite is shown in Figure 4. The LTO/CG composite delivered a capacity of ca. 270 mAh g^{-1} at 25 mA g^{-1} for the two initial cycles, and maintained 210 mAh g^{-1} at 250 mA g^{-1} without any decay for 500 cycles (Figure 4a and b). The results indicate that the LTO/CG composite has excellent cyclic performance, even when using graphene as an active component. Figure 4c and d depict the rate capability of the LTO/CG composite when operating between the cutoffs of 0.01–2.0 V; the capacities are 270, 227, 199, 187, 179, 169, 152, and 117 mAh g^{-1} for the current densities of 25, 50, 125, 250, 500, 1250, 2500, 5000 mA g^{-1}, showing excellent rate capability.[19,21,22,40–42,44] Rarely have LTO/RGO composites been reported upon cycling to the low voltage of 0.01 V. One example of an LTO/RGO anode operated between the cutoffs of 0–2.5 V was reported by Xiang *et al.*[21] The LTO/graphene composite produced by a solvothermal method delivered a capacity of 269 and 228 mAh g^{-1} at the third and 100th cycles (more than 15% decay), respectively. In contrast, our LTO/CG anode had no degradation in capacity for 500 cycles when using the graphene as the active material, further confirming the excellent cyclic capability of the LTO/CG composite.

Figure 4e presents the CV curves of the LTO/CG composite. The LTO/CG was cathodically scanned from an open circuit potential of 3.097 V. The peak at 1.46 V is ascribed to the lithiation of LTO, and the one at 0.73 V is due to the formation of SEI layer on the LTO/CG. The developmental peak below 10 mV is associated with Li ion insertion into graphene. After two cycles between 0.01–1.5 V, the anode was swept between 0.01–2.0 V for two additional cycles, exhibiting a pair of well-overlapping peaks at 1.54/1.66 V, corresponding with the redox reaction between $Li_4Ti_5O_{12}$ and $Li_7Ti_5O_{12}$.[45,46] Note that the irreversible cathodic peak at 0.73 V, related to the SEI formation, was observed only in the first cycle and disappeared in the subsequent cycles at both potential ranges of 0.01–1.5 and 0.01–2.0 V, suggesting that the SEI layer on the graphene is stable. The cation distribution in the $Li_4Ti_5O_{12}$ and $Li_7Ti_5O_{12}$ phases during the charge/discharge process could be expressed as follows:

$$[Li]_{8a}[Li_{1/3}Ti_{5/3}]_{16d}[O_4]_{32e} + Li^+ + e^- \Leftrightarrow [Li_2]_{16c}[Li_{1/3}Ti_{5/3}]_{16d}[O_4]_{32e}. \quad (1)$$

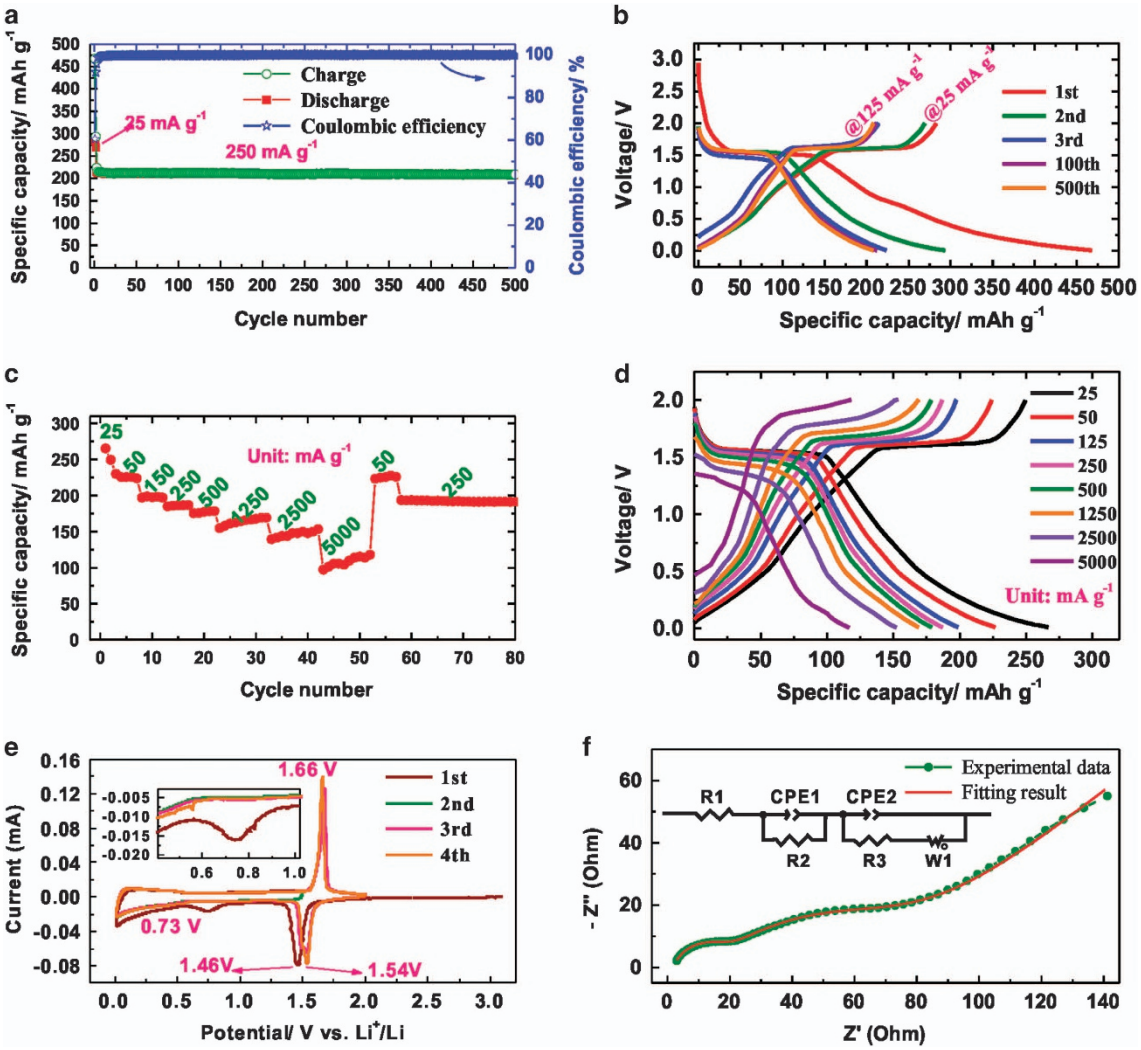

Figure 4 Battery performance and electrochemical characteristics of the LTO/CG anode. Electrochemical performance of the LTO/CG composite within the voltage range of 0.01–2 V: (**a**) cyclic performance at a current density of 250 mA g^{-1} after activation during the initial two cycles at 25 mA g^{-1}, (**b**) charge/discharge curves, (**c**, **d**) rate capability, (**e**) CV curves at a scan rate of 0.05 mV s^{-1}, and (**f**) EIS plot and its fitting results; inset shows the equivalent circuit for fitting. CV, Cyclic voltammetry; EIS, electrochemical impedance spectroscopy; LTO/CG, $Li_4Ti_5O_{12}$/crumpled graphene.

The result is in good agreement with the excellent cyclic performance, as shown in Figure 4a.

As we discussed, the LTO/CG composite prepared with 110% LiOH precursor has some TiO_2 impurities; therefore, we compared the CV results of the LTO/CG with and without TiO_2. The CV behavior (Supplementary Figure S6a) of the LTO/CG composite synthesized in the case of 110% LiOH is quite similar to that using 130% LiOH (Figure 4e), except for a pair of small redox peaks at 1.79/1.98 V (vs. Li^+/Li) due to the TiO_2 impurities. Interestingly, TiO_2 impurities do not significantly affect the performance of LTO/CG anode (Supplementary Figures S6b and c), indicating that the LTO/CG structure is inherently stable during the lithium insertion/extraction process. Figure 4f presents the electrochemical impedance spectroscopy plot of the LTO/CG composite, which uses a two-time-constant equivalent circuit (Figure 4f inset).[47] The Ohmic, SEI layer, charge transfer, and Li ion diffusion resistances are 1.6, 14.8, 66.7, and 265.2 Ω, respectively. The small resistances indicate the excellent conductivity of the LTO/CG composite.

Considering the outstanding performance of the LTO/CG anode in LIBs and the one-step continuous production method, we believe this study offers insight into the development of LTO-based anodes in LIBs. By combing the LTO with high-conductivity nanocarbons of various morphologies, the rate capability and cycling performance of LTO-based anodes could be greatly improved, thereby benefiting the applications of LTO-based LIBs. This study also introduces a new method for the easy preparation of LTO/graphene composites, which may be applicable for producing other anode and cathode materials in LIBs.

CONCLUSION

In summary, we have demonstrated a high-performance LIB anode composed of spherical LTO/graphene composite. The unique 3D and hollow graphene structure greatly increases the conductivity of LTO and facilitates the ion/electron transfer during the charge/discharge process. As the LTO nanocrystals are grown in-situ on the graphene surface, this highly stable structure favors for the long cycle life of the

battery. The batteries using the LTO/CG anode show excellent rate capability and outstanding cycling performance. The battery test confirmed that the LTO/CG structure could effectively overcome the existing challenges of LTO-based anodes and allow for the fabrication of high-capacity and stable anodes with rapid charging capability. Finally, the fabrication method (aerosolization of GO and precursors) is a one-step synthesis method with no need for subsequent treatment of the product and is capable of continuous production, thus offering significant potential for large-scale manufacturing.

CONFLICT OF INTEREST

The authors declare no conflict of interest.

ACKNOWLEDGEMENTS

Financial support for this work was provided by the US National Science Foundation (EECS-1001039 and IIP-1128158) and the Research Growth Initiative Program of the University of Wisconsin-Milwaukee (UWM). The authors thank Professor M. Gajdardziska-Josifovska for TEM access at the high-resolution TEM Laboratory of UWM, Dr. H. A. Owen for technical support with SEM analyses, and Dr. S. E. Hardcastle for technical support with X-ray diffraction, Raman, and thermogravimetric/differential thermal analysis analyses. The SEM imaging was conducted at the Electron Microscope Laboratory of UWM. The X-ray diffraction, Raman, and thermogravimetric/differential thermal analysis were conducted at the Advanced Analysis Facility of UWM.

1 Ji, L., Lin, Z., Alcoutlabi, M. & Zhang, X. Recent developments in nanostructured anode materials for rechargeable lithium-ion batteries. *Energy Environ. Sci.* **4**, 2682–2699 (2011).
2 Armand, M. & Tarascon, J. M. Building better batteries. *Nature* **451**, 652–657 (2008).
3 Tarascon, J. M. & Armand, M. Issues and challenges facing rechargeable lithium batteries. *Nature* **414**, 359–367 (2001).
4 Ganapathy, S. & Wagemaker, M. Nanosize storage properties in Spinel Li4Ti5O12 explained by anisotropic surface lithium insertion. *ACS Nano* **6**, 8702–8712 (2012).
5 Lu, X., Zhao, L., He, X., Xiao, R., Gu, L., Hu, Y. S., Li, H., Wang, Z., Duan, X., Chen, L., Maier, J. & Ikuhara, Y. Lithium storage in Li4Ti5O12 Spinel: the full static picture from electron microscopy. *Adv. Mater.* **24**, 3233–3238 (2012).
6 Yu, L., Wu, H. B. & Lou, X. W. Mesoporous Li4Ti5O12 hollow spheres with enhanced lithium storage capability. *Adv. Mater.* **25**, 2296–2300 (2013).
7 Feckl, J. M., Fominykh, K., Doeblinger, M., Fattakhova-Rohlfing, D. & Bein, T. Nanoscale porous framework of lithium titanate for ultrafast lithium insertion. *Angew. Chem. Int. Ed.* **51**, 7459–7463 (2012).
8 Park, K.-S., Benayad, A., Kang, D.-J. & Doo, S.-G. Nitridation-Driven Conductive Li4Ti5O12 for Lithium Ion Batteries. *J. Am. Chem. Soc.* **130**, 14930–14931 (2008).
9 Amatucci, G. G., Badway, F., Du Pasquier, A. & Zheng, T. An asymmetric hybrid nonaqueous energy storage cell. *J. Electrochem. Soc.* **148**, A930–A939 (2001).
10 Haetge, J., Hartmann, P., Brezesinski, K., Janek, J. & Brezesinski, T. Ordered large-pore mesoporous Li4Ti5O12 spinel thin film electrodes with nanocrystalline framework for high rate rechargeable lithium batteries: relationships among charge storage, electrical conductivity, and nanoscale structure. *Chem. Mater.* **23**, 4384–4393 (2011).
11 Shen, L., Li, H., Uchaker, E., Zhang, X. & Cao, G. General strategy for designing core-shell nanostructured materials for high-power lithium ion batteries. *Nano Lett.* **12**, 5673–5678 (2012).
12 Zhu, G.-N., Wang, Y.-G. & Xia, Y.-Y. Ti-based compounds as anode materials for Li-ion batteries. *Energy Environ. Sci.* **5**, 6652–6667 (2012).
13 Amine, K., Belharouak, I., Chen, Z., Tran, T., Yumoto, H., Ota, N., Myung, S. T. & Sun Y. K. Nanostructured Anode Material for High-Power Battery System in Electric Vehicles. *Adv. Mater.* **22**, 3052–3057 (2010).
14 Guo, J. & Liu, J. Topotactic conversion-derived Li4Ti5O12-rutile TiO2 hybrid nanowire array for high-performance lithium ion full cells. *RSC Adv.* **4**, 12950–12957 (2014).
15 Jo, M. R., Jung, Y. S. & Kang, Y.-M. Tailored Li4Ti5O12 nanofibers with outstanding kinetics for lithium rechargeable batteries. *Nanoscale* **4**, 6870–6875 (2012).
16 Chen, S., Xin, Y. & Zhou, Y. Self-supported Li4Ti5O12 nanosheet arrays for lithium ion batteries with excellent rate capability and ultralong cycle life. *Energy Environ. Sci.* 1924–1930 (2014).
17 Wang, Y.-Q., Gu, L., Guo, Y. G., Li, H., He, X. Q., Tsukimoto, S., Ikuhara, Y. & Wan, L. J. Rutile-TiO2 nanocoating for a high-rate Li4Ti5O12 anode of a lithium-ion battery. *J. Am. Chem. Soc.* **134**, 7874–7879 (2012).
18 Zhao, L., Hu, Y.-S., Li, H., Wang, Z. & Chen, L. Porous Li4Ti5O12 coated with N-doped carbon from ionic liquids for Li-Ion batteries. *Adv. Mater.* **23**, 1385–1388 (2011).
19 Shen, L., Yuan, C., Luo, H., Zhang, X., Yang, S. & Lu, X. In situ synthesis of high-loading Li4Ti5O12-graphene hybrid nanostructures for high rate lithium ion batteries. *Nanoscale* **3**, 572–574 (2011).
20 Jung, H.-G., Myung, S.-T., Son, S.-B., Oh, K. H., Amine, K., Scrosati, B. & Sun, Y.-K. Microscale spherical carbon-coated Li4Ti5O12 as ultra high power anode material for lithium batteries. *Energy Environ. Sci.* **4**, 1345–1351 (2011).
21 Xiang, H., Tian, B., Lian, P., Li, Z. & Wang, H. Sol-gel synthesis and electrochemical performance of Li4Ti5O12/graphene composite anode for lithium-ion batteries. *J. Alloy Compd.* **509**, 7205–7209 (2011).
22 Kim, H. K., Jegal, J.-P., Kim, J.-Y., Yoon, S.-B., Roh, K. C. & Kim, K.-B. In situ fabrication of lithium titanium oxide by microwave-assisted alkalization for high-rate lithium-ion batteries. *J. Mater. Chem. A* **1**, 14849–14852 (2013).
23 Mao, S., Wen, Z., Huang, T., Hou, Y. & Chen, J. High-performance bi-functional electrocatalysts of 3D crumpled graphene-cobalt oxide nanohybrids for oxygen reduction and evolution reactions. *Energy Environ. Sci.* **7**, 609–616 (2014).
24 Mao, S., Wen, Z., Kim, H., Lu, G., Hurley, P. & Chen, J. A general approach to one-pot fabrication of crumpled graphene-based nanohybrids for energy applications. *ACS Nano* **6**, 7505–7513 (2012).
25 Luo, J., Jang, H. D., Sun, T., Xiao, L., He, Z., Katsoulidis, A. P., Kanatzidis, M. G., Gibson, J. M. & Huang, J. Compression and aggregation-resistant particles of crumpled soft sheets. *ACS Nano* **5**, 8943–8949 (2011).
26 Ma, X., Zachariah, M. R. & Zangmeister, C. D. Crumpled nanopaper from graphene oxide. *Nano Lett.* **12**, 486–489 (2012).
27 Ruoff, R. A means to an end. *Nature* **483**, S42–S42 (2012).
28 Luo, J., Jang, H. D. & Huang, J. Effect of sheet morphology on the scalability of graphene-based ultracapacitors. *ACS Nano* **7**, 1464–1471 (2013).
29 Mao, S., Wen, Z., Bo, Z., Chang, J., Huang, X. & Chen, J. Hierarchical nanohybrids with porous cnt-networks decorated crumpled graphene balls for supercapacitors. *ACS Appl. Mater. Interfaces* **6**, 9881–9889 (2014).
30 Choi, S. H. & Kang, Y. C. Fe3O4-decorated hollow graphene balls prepared by spray pyrolysis process for ultrafast and long cycle-life lithium ion batteries. *Carbon* **79**, 58–66 (2014).
31 Choi, S. H. & Kang, Y. C. Crumpled graphene-molybdenum oxide composite powders: preparation and application in lithium-ion batteries. *Chemsuschem* **7**, 523–528 (2014).
32 Choi, S. H., Ko, Y. N., Lee, J.-K. & Kang, Y. C. Rapid continuous synthesis of spherical reduced graphene ball-nickel oxide composite for lithium ion batteries. *Sci. Rep.* **4**, 5786 (2014).
33 Luo, J., Zhao, X., Wu, J., Jang, H. D., Kung, H. H. & Huang, J. Crumpled Graphene-Encapsulated Si Nanoparticles for Lithium Ion Battery Anodes. *J. Phys. Chem. Lett.* **3**, 1824–1829 (2012).
34 Zhou, G.-W., Wang, J., Zhou, G.-W., Gao, P., Yang, X., He, Y.-S., Liao, X.-Z., Yang, J. & Ma, Z.-F. Facile spray drying route for the three-dimensional graphene-encapsulated Fe2O3 nanoparticles for lithium ion battery anodes. *Ind. Eng. Chem. Res.* **52**, 1197–1204 (2013).
35 Ma, X., Zachariah, M. R. & Zangmeister, C. D. Reduction of Suspended Graphene Oxide Single Sheet Nanopaper: The Effect of Crumpling. *J. Phys. Chem. C* **117**, 3185–3191 (2013).
36 Ferrari, A. C., Meyer, J. C., Scardaci, V., Casiraghi, C., Lazzeri, M., Mauri, F., Piscanec, S., Jiang, D., Novoselov, K. S., Roth, S. & Geim, A. K. Raman spectrum of graphene and graphene layers. *Phys. Rev. Lett.* **97**, 187401 (2006).
37 Stankovich, S., Dikina, D. A., Pinera, R. D., Kohlhaasa, K. A., Kleinhammesc, A., Jiac, Y., Wuc, Y., Nguyenb, SB. T. & Ruoffa, S.R Synthesis of graphene-based nanosheets via chemical reduction of exfoliated graphite oxide. *Carbon* **45**, 1558–1565 (2007).
38 Bo, Z., Shuai, X., Mao, S., Yang, H., Qian, J., Chen, J., Yan, J. & Cen, K. Green preparation of reduced graphene oxide for sensing and energy storage applications. *Sci. Rep.* **4**, 4684 (2014).
39 Shi, Y., Wen, L., Li, F. & Cheng, H. M. Nanosized Li4Ti5O12/graphene hybrid materials with low polarization for high rate lithium ion batteries. *J. Power Sources* **196**, 8610–8617 (2011).
40 Chen, W. N., Jiang, H., Hu, Y. J., Dai, Y. H. & Li, C. Z. Mesoporous single crystals Li4Ti5O12 grown on rGO as high-rate anode materials for lithium-ion batteries. *Chem. Commun.* **50**, 8856–8859 (2014).
41 Ni, H. F., Song, W. L. & Fan, L. Z. A strategy for scalable synthesis of Li(4)Ti(5)O(12)/reduced graphene oxide toward high rate lithium-ion batteries. *Electrochem. Commun.* **40**, 1–4 (2014).
42 Tang, Y. F., Huang, F. Q., Zhao, W., Liu, Z. Q. & Wan, D. Y. Synthesis of graphene-supported Li4Ti5O12 nanosheets for high rate battery application. *J. Mater. Chem.* **22**, 11257–11260 (2012).
43 Yang, Y. C., Qiao, B., Yang, X., Fang, L., Pan, C., Song, W., Hou, H. & Xiaobo, J. Lithium titanate tailored by cathodically induced graphene for an ultrafast lithium ion battery. *Adv. Funct. Mater.* **24**, 4349–4356 (2014).
44 Oh, Y., Nam, S., Wi, S., Kang, J., Hwang, T., Lee, S., Park, H. H., Kim, C. & B., Park Effective wrapping of graphene on individual Li4Ti5O12 grains for high-rate Li-ion batteries. *J. Mater. Chem. A* **2**, 2023–2027 (2014).

45 Prakash, A. S., Manikandan, P., Ramesha, K., Sathiya, M., Tarascon, J.- M. & Shukla, A. K. Solution-combustion synthesized nanocrystalline Li4Ti5O12 as high-rate performance Li-Ion battery anode. *Chem. Mater.* **22**, 2857–2863 (2010).
46 Wagemaker, M., Simon, D. R.., Kelder, E. M., Schoonman, J., Ringpfeil, C., Haake, D., Lützenkirchen-Hecht,, D. & Frahm, F. M. A kinetic two-phase and equilibrium solid solution in spinel Li4+xTi5O12. *Adv. Mater.* **18**, 3169–3173 (2006).
47 Huang, X. K., Yang, J., Mao, S., Chang, J., Hallac, P. B., Fell, C. R., Metz, B., Jiang, J., Hurley, P. T. & Chen, J. Controllable synthesis of hollow Si anode for long-cycle-life lithium-ion batteries. *Adv. Mater.* **26**, 4326–4332 (2014).

Supplementary Information accompanies the paper on the NPG Asia Materials website (http://www.nature.com/am)